

A. ŻYRA^{*#}, R. BOGUCKI^{**}, S. SKOCZYPIEC^{*}

AN INFLUENCE OF TITANIUM ALLOY Ti10V2Fe3Al MICROSTRUCTURE ON THE ELECTRODISCHARGE PROCESS EFFICIENCY

In the work results of research on electrodischarge machining (EDM) of titanium alloy Ti10V2Fe3Al with ($\alpha + \beta$) structure were presented. Preliminary heat treatment of samples allows to obtain different morphology and volume fraction of the α phase. The main goal of research was to assessment of the material microstructure impact on EDM technological factors (ie. material removal rate, tool wear) and morphology of technological surface layer. Electrodischarge machining is alternative and increasingly used method of titanium alloys machining. Research allowed to indicate the possibilities and limitations of use EDM in this area. It is especially important in the aspect of parts produced for aircraft industry and related requirements for the technological surface layer quality.

Keywords: electrodischarge machining (EDM), microstructure, Ti10V2Fe3Al alloy, Titanium Grade 2

1. Introduction

The high mechanical properties of titanium alloys are a good alternative to structural steels for constructional applications. Titanium alloys are characterized by a high ratio of strength to specific weight, hence they are used in the aerospace industry. Modification of the chemical composition and the use of thermo – mechanical treatment and heat treatment enable reaching a similar level of strength as in high-strength construction steels. Titanium alloys can be characterized by single-phase (α or β) and biphasic ($\alpha + \beta$) structure [1-4]. The volume fraction of the α and β phases can be controlled by the chemical composition of the titanium alloy and the heat treatment applied. The highest strength properties are characterized by $\alpha + \beta$ structure, in which the β phase is stabilized by the use of alloying elements such as V, Mo, Fe [5-7]. It was observed that the Ti10V2Fe3Al alloy can be characterized by different morphology and volume fraction of the α by controlling the temperature and time of heat treatment. Annealing in the ($\alpha + \beta$) range leads to obtaining globular precipitates of the alpha phase, and the volume fraction is controlled by temperature and time [5,8-10]. The use of titanium heat treatment with preheating above the $\alpha \rightarrow \beta$ transformation with subsequent cooling to the ($\alpha + \beta$) range results in the precipitates of the needles alpha phase, and their volume fraction also depends on the temperature and time of annealing [9,10].

The limited use of titanium alloys is the result of the high costs of their production and processing (cost of manufactur-

ing can reach 50% of total part cost). Traditional machining by cutting is particularly cost-intensive due to the low thermal conductivity of titanium. This leads to accelerated tool wear and poor cutting performance. An important problem particularly noticeable in the aviation industry is also high material losses during machining [11]. An alternative to traditional machining methods used for hard to machine materials, such as titanium alloys is electrodischarge machining (EDM). One of the most important advantage is that EDM enables to machine each type of material which is electrical conductor or semi-conductor regardless of its mechanical properties or chemical composition [12-13]. Electrodischarge machining is an electro-thermal process. The material removal takes place as a result impulsive electrical discharges in narrow gap ($<100 \mu\text{m}$) between working electrode and workpiece immersed in dielectric liquid. Due to interaction with plasma channel which occurs in the gap the machined material's is melted and evaporated. In the working area the forced flow of dielectric liquid enables efficient removing of resolidified material's particles [12,14-16]. It also disperses heat generated during the process, what allows to workpiece and electrode tool surface cooling [17]. The most commonly used dielectrics are: water based and carbon based dielectric liquids [18].

Efficiency of EDM is strongly connected with thermal and electrical properties of machined material. During the process high amount of energy from electrical discharges is delivered to the machining area. The generated energy depends except material's electrical and thermal properties also on setting

* CRACOW UNIVERSITY OF TECHNOLOGY, DEPARTMENT OF MECHANICAL ENGINEERING, INSTITUTE OF PRODUCTION ENGINEERING, AL. JANA PAWŁA II 37, 31-864, KRAKÓW, POLAND

** CRACOW UNIVERSITY OF TECHNOLOGY, DEPARTMENT OF MECHANICAL ENGINEERING, INSTITUTE OF MATERIALS SCIENCE, AL. JANA PAWŁA II 37, 31-864, KRAKÓW, POLAND

Corresponding author: agazyra@gmail.com

proper machining (electrical) parameters such as pulse time, pause time, gap voltage and current amplitude. Only small part of this energy (about 1%) is responsible for workpiece material removal [14]. Majority of discharge energy has to be effectively dispersed from the gap (mainly via conduction through electrode or tool material), therefore the material's heat absorption and dissipation capabilities are important factor of process reliability. Due to specific characteristics of titanium alloys (high melting temperature, low electrical resistance and high heat resistance) it is impossible to apply the same machining strategy which are well known and commonly used for most of the metals machined by EDM. What is more there are no available and universal combination of parameters which enable to gain assumed results. The Ti-6Al-V4 electrical resistivity is two and a half times higher comparing to steel 304L and increases with the temperature [19-21].

To sum up, in the context of titanium alloys EDM machining, the effective heat dissipation from the machining gap is crucial, since even slight disturbance in the machining parameters can affect the process stability and as a result machined surface integrity, shape and dimensional accuracy of machined part [20-22].

2. Material and method

The investigations were carried out on the titanium alloy Ti10V2Fe3Al samples which was delivered in the form of forgings taken from one casting with thickness 30 mm. In addition, Titanium Grade 2 characterized by the alpha matrix was analysed. The chemical composition of the alloys are given in Table 1. The temperature of β transformation of this alloy is 828°C. The process of thermo-mechanical treatment was carried out in two stages. The preliminary forging process of Ti10V2Fe3Al was carried out in the β range at the temperature

of 900°C. The second forging step was performed at 750°C in the $\alpha + \beta$ range.

In order to obtain the two-phase $\alpha + \beta$ Ti10V2Fe3Al structure with different volume fraction and morphology of the α phase precipitates, two heat treatment procedures were carried out [9]. The heat treatment was carried out in a Nabertherm P330 tubular furnace under an Ar atmosphere, according to two schemes. In Scheme I $\beta + (\alpha + \beta)$, initial heating was applied to 900°C, at a rate of 10°C/min, followed by annealing for 20 min. The samples were then cooled in an oven at a rate of 10°C/min. to 700°C, and annealed for 15, 30, 60 min. and then cooled in water. In Scheme II ($\alpha + \beta$) the samples were heated to 700°C, at a rate of 10°C/min and heated for 15, 30, 60 min and cooled in water.

The temperatures of individual heat treatments and the annealing time with the corresponding volume fraction of the α phase are shown in Table 2. The preparation of sample surfaces for the electrical discharge machining consisted of mechanical grinding and polishing. Then, to reveal the microstructure, the samples were chemically etched in the solution containing 10 ml HNO₃ + 20 ml HF + 20 ml glycerine. Observations of the microstructure were performed using optical microscope Nikon ME 60 and scanning electron microscope JOEL JSM5510LV. The stereological calculations of the volume fraction of the α phase were performed using Image J software at a total analysis area of 1 mm².

Then, EDM drilling tests were carried out on a research test stand equipped with electrodischarge generator BP 95, manufactured by a Polish company ZAP B.P. Końskie-Kutno. On the each sample the influence of current amplitude (5, 10 and 15 A) on the surface layer condition, material removal rate and tool wear were investigated.

Other machining parameters (see Table 3) were selected in preliminary tests and allows to stabilize EDM machining process with the applied electrical generator. As dielectric hydrocarbon fluid was chosen. It is the most commonly used type of dielectric

TABLE 1

Chemical composition and thermal properties of investigated materials

Material	V	Al	Fe	O	N	C	Ti	Thermal conductivity [W/m·°C]	Electrical resistance [μOhm/m]
Ti10V2Fe3Al	9.9	2.9	1.9	0.13	0.007	0.002	Bal.	16.4	0.5
Titanium Grade 2	—	—	0.3	0.25	0.003	0.1	Bal.	~7	~1.7

TABLE 2

The temperatures of individual samples heat treatments and the annealing time with the corresponding volume fraction of the α phase

Temperature domain	Time of soaking [min]	Morphology and volume fraction of α phase	Sample number
$(\alpha + \beta)$ 750°C	120	globular: ~25%	1G
	30	globular: ~38%	2G
	5	globular: ~46%	3G
$\beta + (\alpha + \beta)$ 900°C + 700°C	15	acicular: ~18%	4A
	30	acicular: ~48%	5A
	60	acicular: ~62%	6A

for EDM sinking. Additionally, in case of investigated material machining with hydrocarbon based dielectric is safe, because no vanadium oxides are generated during the process. To characterise EDM machinability for each sample (material composition) the test with the central current intensity value ($I = 10$ A) was carried out for 60 min. The tests were carried out in kinematics of sinking with application of cylindrical copper electrode tool with outer diameter 5 mm. Electrode tool was changed after each probe what allows also to analyse electrode tool wear. During the tests reverse polarity (working electrode (+), workpiece (-)) was applied. Detailed machining conditions were summarised in the Table 3.

TABLE 3

Sinking EDM machining conditions and output factors

Workpiece material	Ti10V2Fe3Al, Titanium Grade 2			
Working electrode	thin-walled cooper pipe electrode, outer diameter \varnothing 5 mm			
Dielectric	Exsoll D80			
Current intensity [A]	5	10	15	10
Machining time [min]	5	5	5	60
Current voltage [V]	240			
Pulse on-time [μ s]	100			
Pulse off-time [μ s]	50			
Auto – reg.	0N			
Polarity	working electrode (+), workpiece (-)			
Output factors	surface integrity, working electrode wear, material removal rate			

3. Results and discussion

3.1. Microstructure

The phase composition of the analyzed alloy was confirmed by x-ray examinations. The analysis was carried out for sample 2G with globular particles and for sample 5A with acicular particles (see Fig. 1a and Fig. 1b). Diffractograms confirmed the presence of phase α and β in the titanium structure. In the case of sample 2G, there is a slight shift of peaks which is the result of cumulative plastic deformation in the sample after the forging process.

The applied heat treatment schemes lead to different morphology and volume fraction of α phase. Globular particles of the Ti10V2Fe3Al α phase in the β -matrix were obtained after annealing below $\alpha \rightarrow \beta$ transformation, at a temperature of 750°C in the ($\alpha + \beta$) range. The increase in the annealing time leads to a decrease in the volume fraction of the globular α -phase. Annealing for 5 min at 750°C resulted in 46% of the globular phase α , extending the time to 120 min caused a decrease in the volume fraction to the level of 25% (Fig. 2). Samples heated at 750°C for 5 min retain the deformed grains of the β -phase, which was formed during the forging process. This indicates that there is no recrystallization process during annealing after 120 min. The signs of the titanium β matrix recovery process were also

After each 60 min ($I = 10$ A) probe of the sample and working electrode were weighted to define the material removal rate as well as working electrode wear. Additionally the surface layer quality of each drilled hole in the samples' were investigated. To identify the structural and morphological changes in the material layer adjacent to machined surface of drilled holes, as well as to identify the machining accuracy by holes edges' quality analysis, the SEM photos were taken.

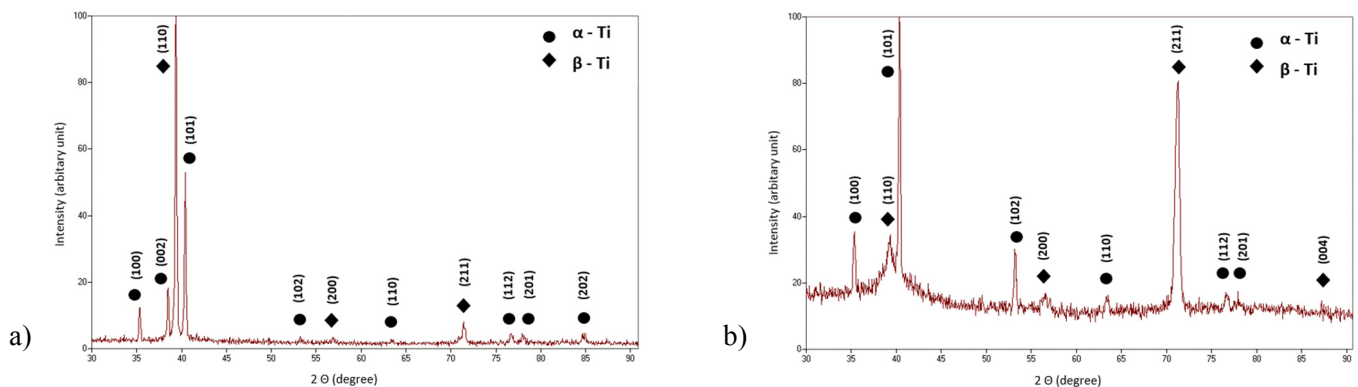


Fig. 1. Diffraction pattern for the as-received Ti10V2Fe3Al. Reflections from phase α and β have been identified, a) sample 2G, b) sample 5A

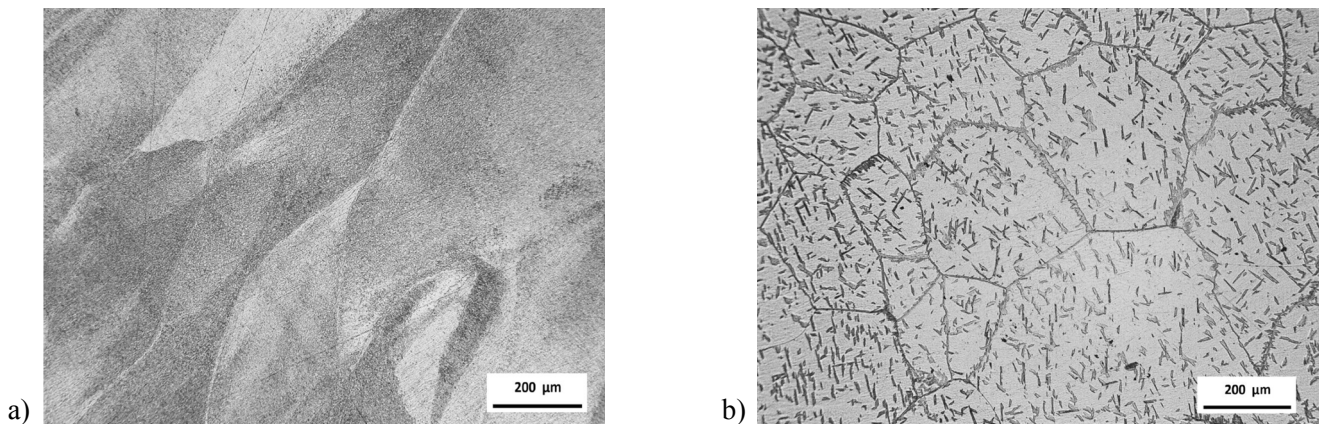


Fig. 2. Optical micrographs of specimen after heat treatment: a) deformed β -phase grains (750°C 5 min), 3G sample, b) recovery processes of the β -phase grains (900°C/700°C 15 min), 4A sample

observed (Fig. 3). The second heating scheme ($\beta + (\alpha + \beta)$) caused the precipitation of the α -phase particles in the form of needles. The first stage of heat treatment consisted of heating above the transformation $\alpha \rightarrow \beta$, to a temperature of 900°C. This led to the dissolution of the α -phase and obtaining a homogeneous β solid solution. Cooling with the furnace to 700°C, below the β -transformation, began the process of precipitation of the α -phase, which nucleated inside the grains and at the grain boundaries of the β -phase (Fig. 4). The amount of α -phase formed is dependent on the annealing time. After heating for 15 minutes, the proportion of α -phase at 18% was obtained. Extending the time to 120 minutes resulted in an increase in the volume fraction of α -phase to 62%. A recrystallized β -matrix was observed for all annealing times. Table 2 summarizes the results of volume fraction measurement of the α phase.

3.2. EDM machining

During the tests (Fig. 5 and Fig. 6) it was found that EDM drilling with described above parameters in hydrocarbon dielectric liquid was quite stable process. Even that, the increase of workpiece temperature was observed. It was noticed that there

are slight differences between material removal rate comparing samples ($\alpha + \beta$) and $\beta + (\alpha + \beta)$. The lowest MRR was found for 4A sample (0.4 cm³/min) and the highest for Titanium Grade 2 sample (0.48 cm³/min). The highest MRR of Titanium Grade 2 sample is connected with its higher thermal conductivity and lower electrical resistance comparing with grade 5 structure at the rest of samples (see Table 2). It is possible to see in the Fig. 5 the increase of MRR with the increase amount of α structure in both group of samples, however the differences between MRR values are to slight. It shows the necessarily to undertake the further tests in this area. Also similar working electrode wear was observed for each sample during tests (Fig. 6). It confirms stability of the process, the ER wear was relatively small. The highest EW was noticed for Titanium Grade 2 sample (3.5%).

Observations of the machined surface revealed the occurrence of characteristic craters after the discharge process. Surface microcracks are visible. It has also been observed that there are deeper openings which may indicate a stronger dissolution of the material. This may be due to the metastable β phase. It has been found that strain-induced martensitic transformation is observed in the analysed titanium alloy with a low alpha volume fraction [9,10]. However, this requires further research and observation.

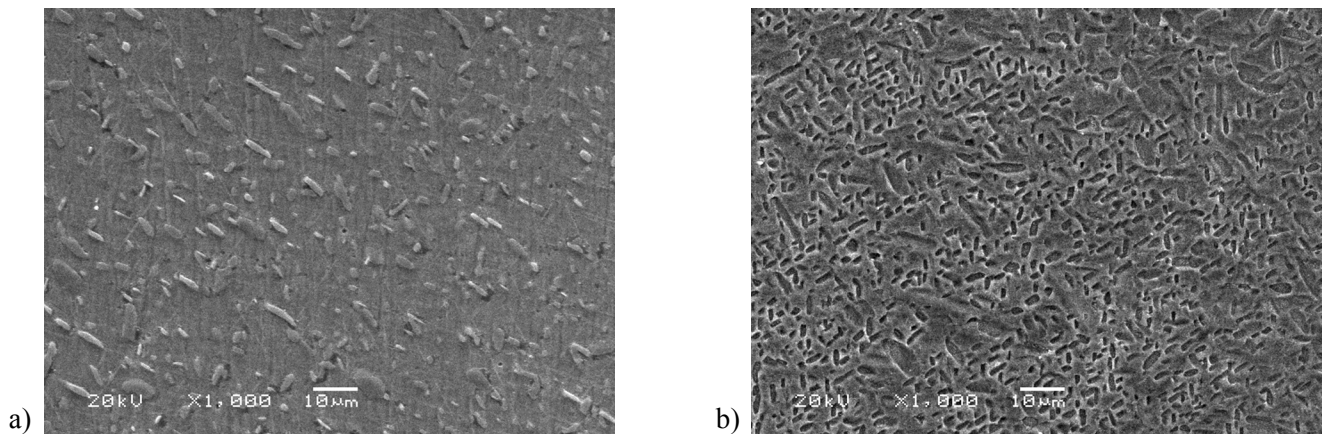


Fig. 3. SEM micrographs of specimens after heat treatment: a) globular α phase in β matrix (750°C 120 min), 1G sample, b) globular α phase and β matrix (750°C 5 min), 3G sample

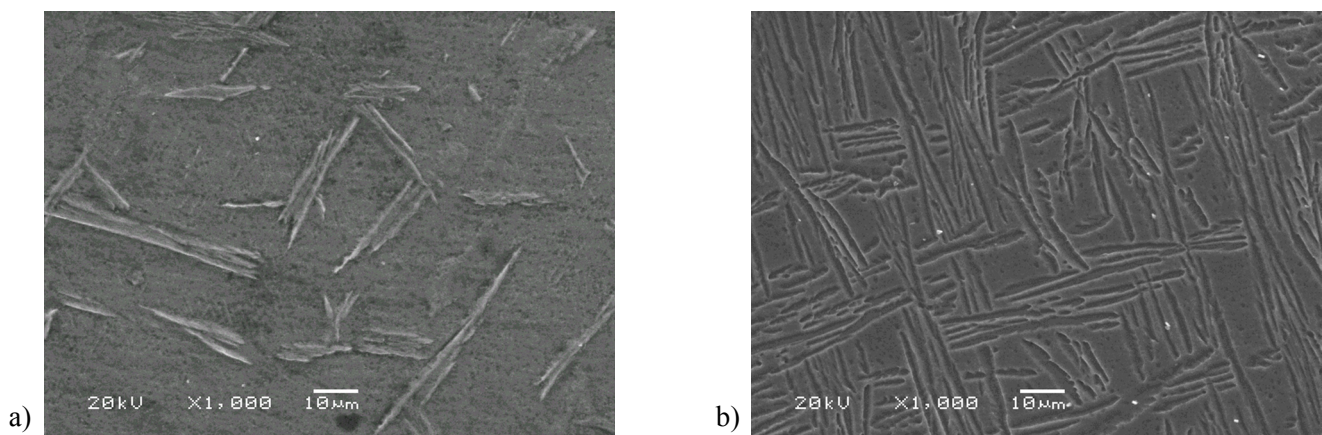


Fig. 4. SEM micrographs of specimens after heat treatment: a) acicular α phase in β matrix (900/700°C 15 min), 4A sample, b) acicular α phase and β matrix (900/700°C 60 min), 6A sample

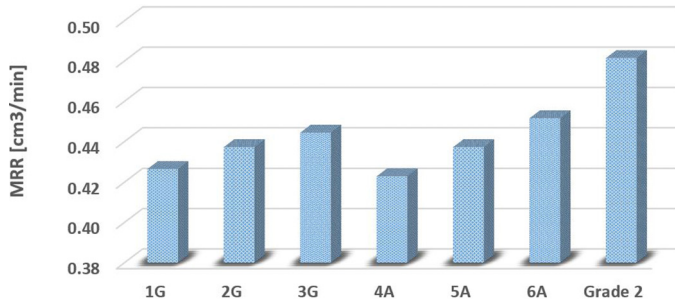


Fig. 5. Comparison of material removal rate (MRR) for Ti10V2Fe3Al and Grade 2 sample EDM drilling carried out in the Exsoll D80, current intensity =10 A, machining time = 60 min

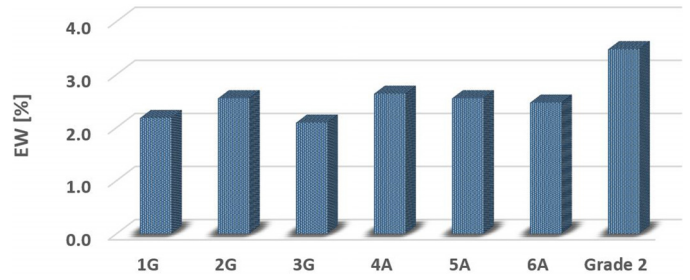


Fig. 6. Comparison of tool wear (EW) for Ti10V2Fe3Al and Grade 2 sample EDM drilling carried out in the Exsoll D80, current intensity =10 A, machining time= 60 min

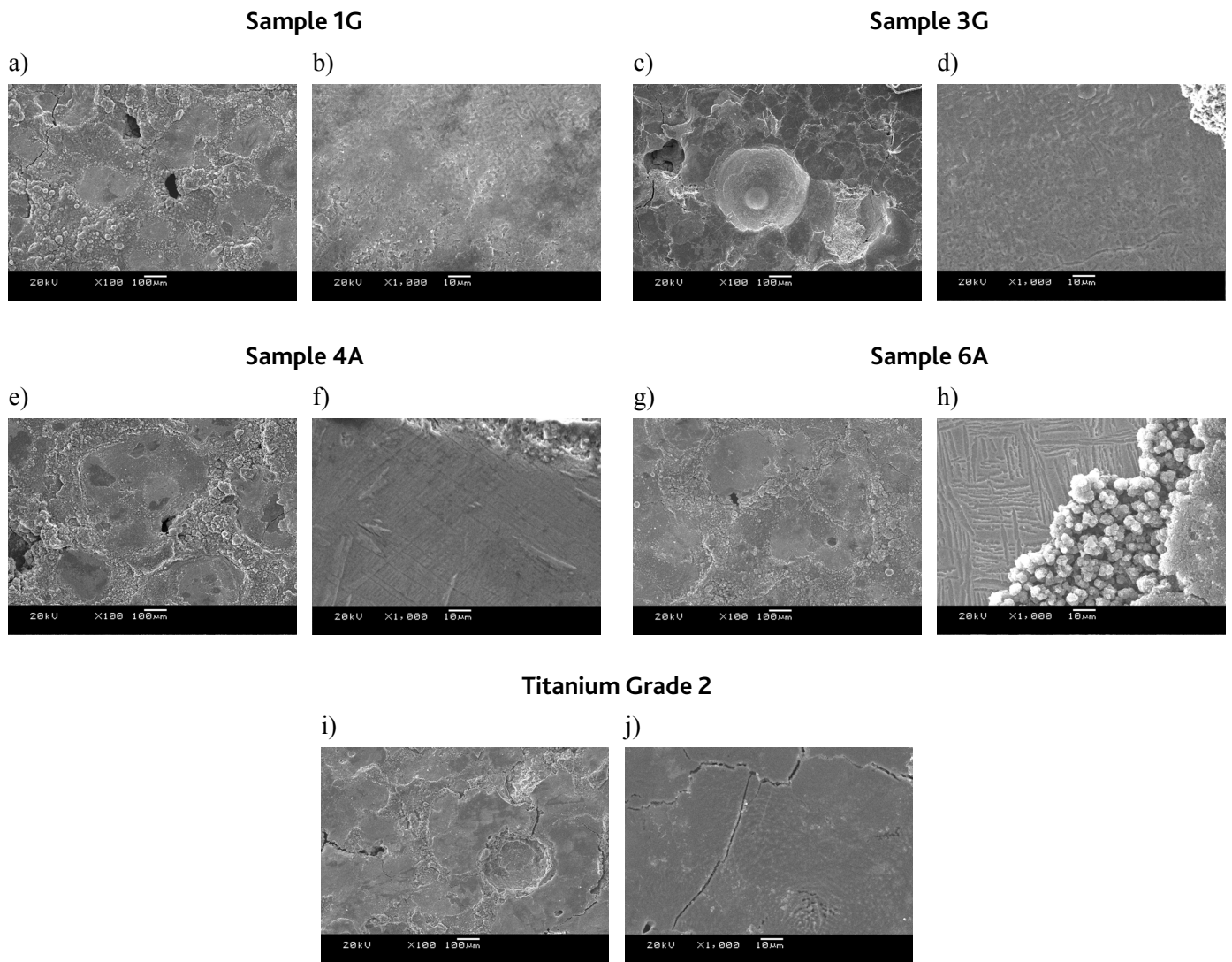


Fig. 7. SEM observation of the surface after EDM machining and microstructure at the machined edge. Parameters of EDM, I=10 A, U=240 V, machining time= 60 min. Micrographs: a), c), e), g), i) surface condition after processing, b), d), f), h), j) microstructure at the machined edge

Observations of the microstructure did not reveal changes in the drill. This shows that the amount of heat is small and the EDM process does not lead to a change in the morphology and volume fraction of the alpha phase of Fig. 7. This is particularly evident in samples with a low volume fraction of α phases, Fig. 7b and Fig. 7f.

4. Conclusions

1. The increase in the volume fraction of alpha phase in the microstructure leads to a slight growth in MRR.
2. The highest MRR value was obtained for the Titanium Grade 2 with an α matrix, with the highest electrode wear at the same time.

3. Changes in the microstructure at the nearby drilled hole edge were not observed.
4. Observed increase of MRR is thought to be connected with the increase of alpha phase in the machined materials and at the same time with the decrease of heat resistance.

REFERENCES

- [1] T.W. Duerig, J. Albrecht, D. Richer, P. Fischer, *Acta Metall.* **30**, 2161-2172 (1982)
- [2] R. Dąbrowski, *Arch. Metal. Mater.* **56**, 217-221 (2011).
- [3] R. Dąbrowski, *Arch. Metal. Mater.* **56**, 703-707 (2011).
- [4] G. LüterIng, J.C. Williams, *Titanium*, second ed., Springer, Berlin, 2007.
- [5] Z. Wyatt, S. Ankem, *J. Mater. Sci.* **45**, 5022-5031 (2010).
- [6] C. Ouchi, H. Fukai, K. Hasegawa, *Mater. Sci. Eng. A* **263**, 132-136 (1999).
- [7] T. Grosdidier, Y. Combress, E. Gautier, M.J. Philippe, *Metall. Mater. Trans. A* **31A**, 1095-1106 (2000).
- [8] W. Xu, K.B. Kim, J. Das, M. Calin, J. Eckert, *Scripta Mater.* **54**, 1943-1948 (2006).
- [9] R. Bogucki, K. Mosór, M. Nykiel, *Arch. Metal. Mater.* **59**, 1269-1273 (2014).
- [10] C. Li, X. Wu, J.H. Chen, S. Vander Zwaag, *Mater. Sci. Eng. A* **528**, 5854-5860 (2011).
- [11] W. Zębala, J. Gawlik, A. Matras, G. Struzikiewicz, Ł. Ślusarczyk, *Precision Machining VII* **581**, 409-414 (2014).
- [12] B. B. Pradhan, M. Masanta, B. R. Sarkar, B. Bhattacharyya, *International Journal of Advanced Manufacturing Technology* **41**, 11-12, 1094-1106 (2009).
- [13] Y. Zhang, Y. Liu, Y. Shen, R. Ji, Z. Li, C. Zheng, *Journal of Materials Processing Technology* **214**, 5, 1052-1061 (2014).
- [14] M. Kunieda, B. Lauwers, K.P. Rajurkar, B.M. Schumacher, *CIRP Annals - Manufacturing Technology* **54**, 2, 64-87 (2005).
- [15] A. Goodlet, P. Koshy, *CIRP Annals – Manufacturing Technology* **64**, 1, 241-244, 2015.
- [16] F. Klocke, L. Hensgen, A. Klink, L. Ehle, A. Schwedt, *Process, Procedia CIRP* **42**, 673-678 (2016).
- [17] A. Żyra, W. Bizoń, S. Skoczypiec, *Primary Research On Dry Electrodischarge Machining With Additional Workpiece Cooling*, no. 2.
- [18] A. Żyra, R. Bogucki, S. Skoczypiec, *Technical Transactions no. Y. 114*, **12**, 231-242 (2017).
- [19] W.J. Zhang, B.V Reddy, S.C. Deevi **45**, 645-651 (2001).
- [20] M. Zhang, Q. Zhang, G. Zhu, Q. Liu, J. Zhang, *Effects of Some Process Procedia CIRP* **42**, 627-631 (2016).
- [21] P. Fonda, Z. Wang, K. Yamazaki, Y. Akutsu, *Journal of Materials Processing Technology* **202**, 1-3, 583-589 (2008).
- [22] M.A.R. Khan, M.M. Rahman, *International Journal of Advanced Manufacturing Technology* **92**, 1-4, 1-13 (2017).